Katholieke Universiteit Leuven

Departement Elektrotechniek ESAT-SISTA/TR 09-207

Comparative evaluation of howling detection criteria in notch-filter-based howling suppression[1]

Toon van Waterschoot[2] [3] and Marc Moonen[2]

November 2010
Published in *Journal of the Audio Engineering Society*, vol. 58, no. 11, Nov. 2010, pp. 923–940.

[1]This report is available by anonymous ftp from *ftp.esat.kuleuven.be* in the directory *pub/sista/vanwaterschoot/reports/09-207.pdf*

[2]K.U.Leuven, Dept. of Electrical Engineering (ESAT), Research group SCD(SISTA), Kasteelpark Arenberg 10, 3001 Leuven, Belgium, Tel. +32 16 321927, Fax +32 16 321970, WWW: *http://homes.esat.kuleuven.be/∼tvanwate*. E-mail: *toon.vanwaterschoot@esat.kuleuven.be*.

[3]This research work was carried out at the ESAT Laboratory of Katholieke Universiteit Leuven, in the frame of K.U.Leuven Research Council CoE EF/05/006 (“Optimization in Engineering, OPTEC”), the Belgian Programme on Interuniversity Attraction Poles initiated by the Belgian Federal Science Policy Office IUAP P6/04 (DYSCO, “Dynamical systems, control and optimization”, 2007-2011), the Concerted Research Action GOA-AMBioRICS, and Research Project FWO nr. G.0600.08 (“Signal processing and network design for wireless acoustic sensor networks”), and was supported by the Institute for the Promotion of Innovation through Science and Technology in Flanders (IWT-Vlaanderen). The scientific responsibility is assumed by its authors.

Comparative Evaluation of Howling Detection Criteria in Notch-Filter-Based Howling Suppression

Toon van Waterschoot and Marc Moonen *AES Associate Member*

(toon.vanwaterschoot@esat.kuleuven.be) (marc.moonen@esat.kuleuven.be)

Department of Electrical Engineering, ESAT-SCD, Katholieke Universiteit, Leuven, B-3001 Leuven, Belgium

Notch-filter-based howling suppression (NHS) is a popular approach to acoustic feedback control in public address and hands-free communication systems. The NHS method consists of two stages: howling detection and notch filter design. While the design of notch filters is well established, there is little agreement in the NHS literature on how the detection problem should be tackled. Moreover since the NHS literature consists mainly of patents, only few experimental results have been reported. A unifying framework for howling detection is provided and a comparative evaluation of existing and novel howling detection criteria is performed.

INTRODUCTION

The acoustic feedback problem is a long-standing problem appearing in sound reinforcement systems such as public address and hands-free communication systems. When a sound signal is captured by a microphone, and subsequently amplified and played back through a loudspeaker, the loudspeaker sound is often fed back to the microphone either through a direct acoustic coupling or indirectly as a result of reverberation. The existence of such an acoustic feedback path results in a closed signal loop, which limits the performance of a sound reinforcement system in two ways. First there is an upper limit to the amount of amplification that can be applied if the system is required to remain stable, which is referred to as the maximum stable gain (MSG). Second the sound quality is affected by occasional howling when the MSG is exceeded or, even when the system is operating below the MSG, by ringing and excessive reverberation.

State-of-the-art methods for acoustic feedback control can be categorized into four classes [1]: phase modulation methods, gain reduction methods, spatial filtering methods, and room modeling methods. Gain reduction is without any doubt the most widespread method for acoustic feedback control in sound reinforcement systems, where the actions that a human operator would undertake for preventing or eliminating howling in a sound reinforcement system are automated. These actions usually consist in reducing the electroacoustic forward path gain, such that the system moves away from the point of instability. Depending on the width of the frequency band in which the gain is actually reduced, we can discriminate between three gain reduction methods [1]. In automatic gain control (AGC) methods [2]–[4], the gain is reduced equally in the entire frequency range, whereas in automatic equalization (AEQ) methods [4]–[10] a gain reduction is applied only in critical subbands (subbands in which the loop gain of the sound reinforcement system is close to unity). In notch-filter-based howling suppression (NHS) methods [11]–[25] the gain is reduced in narrow frequency bands around critical frequencies (frequencies at which the loop gain is close to unity).

Every gain reduction method has to be activated in some way when a closed-loop instability or a tendency toward instability is detected. Most gain reduction methods are reactive, in the sense that howling can usually be perceived before it can actually be detected by a howling detection device or algorithm. In these methods howling detection is typically based on a combined spectral and temporal analysis of the microphone signal. Due to the sinusoidal nature of howling, the microphone signal frequency components having the largest magnitude are considered to be candidate howling components. The true howling components within this set of candidates can then be discriminated from the source signal tonal components (originating from voiced speech or musical tones) using several criteria. Spectral criteria for discriminating between howling and tonal components may be based on one or more of the following features: the power ratio of the candidate howling component and the entire spectrum [5]–[7], [14]–[16], [18]–[25], the power ratio of the candidate howling component and its (sub)harmonics [12]–[15], [17], and the power ratio of the candidate howling component and its neighboring frequency components [4], [8]–[10]. On the other hand temporal criteria for howling detection rely on the observation that howling components typically persist for a longer time than tonal components [2], [3], [11]–[13], [16]–[21] and exhibit an exponentially increasing magnitude until the sound reinforcement system saturates [8]–[10].

*Presented at the 126th Convention of the Audio Engineering Society, Munich, Germany, 2009 May 7–10; revised 2009 October 12 and 2010 June 22.

The goal of this paper is twofold. First we aim to evaluate existing howling detection criteria in an objective way. This can be achieved by reformulating the howling detection problem as a binary hypothesis test and hence evaluating the detection performance using standard measures from detection theory, such as the receiver operating characteristic (ROC) curve [26, ch. 3]. Such an evaluation has not been reported earlier and is necessary to make a fair comparison between existing howling detection methods and to highlight their shortcomings. A second goal consists in the development of novel howling detection criteria that are particularly suited for audio applications involving music signals. In [1] it was found that most of the existing howling detection criteria suffer from an intolerably high probability of false alarm when the microphone signal is a music signal. This is due to the fact that it is much harder to discriminate howling components from tonal audio components in music than from voiced speech components. False alarms result in the unnecessary activation of notch filters, which can be detrimental for the sound quality [1].

The paper is organized as follows. In Section 1, we outline the NHS method for acoustic feedback control, which consists of two stages: howling detection and notch filter design. Six microphone signal features that have been proposed for howling detection are then defined in a formal way in Section 2. These features are used in Section 3 to rederive existing howling detection criteria, and to develop novel howling detection criteria. Both the existing and novel howling detection criteria are then objectively evaluated and compared, and appropriate values for the detection thresholds are suggested. In Section 4, a selection of the existing and novel howling detection criteria are applied in an NHS computer simulation to assess the acoustic feedback control performance in terms of achievable amplification, sound quality, and reliability. Finally Section 5 concludes the paper. We note that while the focus of this paper is on NHS methods, the proposed howling detection criteria can also be applied to other gain reduction methods such as AGC and AEQ.

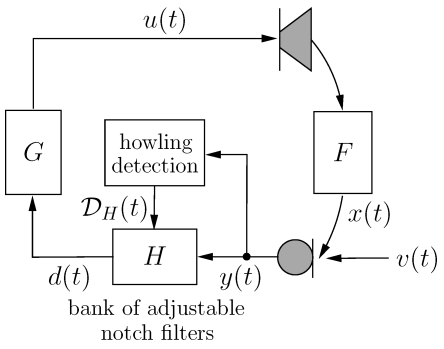

Fig. 1. Notch-filter-based howling suppression (NHS) by feeding microphone signal to a howling detection algorithm, which forwards a set of design parameters $\mathcal{D}_H(t)$ to a bank of adjustable notch filters $H(q, t)$ inserted in electroacoustic forward path.

1 NOTCH-FILTER-BASED HOWLING SUPPRESSION

The NHS method for acoustic feedback control can be outlined as shown in Fig. 1 for a sound reinforcement system with one loudspeaker and one microphone. Here $F(q, t)$ and $G(q, t)$ denote the transfer functions of the acoustic feedback path and the electroacoustic forward path, respectively, with q the time shift operator: $q^{-k}u(t) = u(t - k)$. The source signal $v(t)$ is picked up by the microphone, together with the feedback signal $x(t) = F(q, t)u(t)$. The resulting microphone signal $y(t) = v(t)+x(t)$ is subsequently amplified and processed in the electroacoustic forward path to yield the loudspeaker signal $u(t) = G(q, t)y(t)$. In the NHS method the microphone signal $y(t)$ is also processed by a howling detection algorithm, which forwards a set of design parameters $\mathcal{D}_H(t)$ to a bank of adjustable notch filters $H(q, t)$ that is inserted in the electroacoustic forward path such that $u(t) = H(q, t)G(q, t)y(t)$. The concept of howling detection and notch filter design is described next, closely following [1].

1.1 Howling Detection

We assume that the howling detection is performed in a frame-based manner, on microphone signal frames with a frame length of M samples and a frame hop size of P samples (that is, a frame overlap of $M - P$ samples). At time t the data in the microphone signal frame can then be represented by the vector

$$\mathbf{y}(t) = [y(t + P - M) \cdots y(t + P - 1)]^{\mathrm{T}} \tag{1}$$

and the short-term microphone signal spectrum can be obtained as the discrete Fourier transform (DFT) of the data in $\boldsymbol{y}(t)$, namely,

$$Y(\omega_k, t) = \sum_{n=0}^{M-1} w(t_n)y(t_n)\mathrm{e}^{-\mathrm{j}\omega_k t_n}, \quad k = 0, \ldots, M-1 \tag{2}$$

with $\omega_k \triangleq 2\pi k/M$ and $t_n \triangleq t + P - M + n$. The microphone signal DFT in Eq. (2) is generally calculated using the fast Fourier transform (FFT) algorithm and includes a window function $w(t_n)$ to reduce the spectral leakage [27]. For example, a Blackman window has been applied successfully to audio signal processing [28].[1] The choice of the signal framing parameters M and P has a rather profound influence on the performance of the howling detection. Small values for the frame length M have been proposed to allow for very quick howling detection (for example, $M = 128$, corresponding to 4 ms at $f_s = 32$ kHz [8]–[10]), such that howling may potentially

[1] http://ccrma.stanford.edu/~jos/mdft/Use_Blackman_Window.html.

be detected before it is actually perceived [8]–[10]. On the other hand larger values for M provide a better frequency resolution in the microphone signal DFT spectrum estimate (such as $M = 4096$, corresponding to 92.9 ms at $f_s = 44.1$ kHz [12], [13] or to 85.3 ms at $f_s = 48$ kHz [19], [20]), which is necessary when working with very narrow-band notch filters such as the 1/60 octave filters used in [22], [23]. A large frame hop size P may result in a large time lag between howling detection and notch filtering, unless a P-sample delay is inserted in the electroacoustic forward path. On the other hand a small value for P leads to an increase in computational complexity since the howling detection algorithm is then executed more often. In general, a 25–50% frame overlap ($P = 3M/4, \ldots, M/2$) is found to be a good compromise. In the sequel we will always work with $M = 4096$ and $P = M/2 = 2048$ at a sampling frequency $f_s = 44.1$ kHz.

A predefined number N of spectral peaks is identified from the DFT magnitude spectrum estimate, with N typically chosen in the range of 1–10. These N frequency components are termed "candidate howling components" and their angular frequency values are collected in the set $\mathcal{D}_{\breve{\omega}}(t) = \{\breve{\omega}_i\}_{i=1}^{N}$. A spectral peak picking algorithm (see, for example, [29]) is usually applied to find the candidate howling components. A more advanced approach consists in selecting frequency components that have a consistently increasing magnitude in successive signal frames. This is possible by applying a so-called ballistics procedure [19], [20] before executing the peak picking algorithm. A number of spectral and temporal features are then calculated and combined in a howling detection criterion to determine whether a candidate howling component indeed corresponds to a howling component or rather to a source signal tonal component; see Sections 2 and 3 for more details. The complete howling detection procedure is summarized in Fig. 2.

1.2 Notch Filter Design

When howling has been detected, a notch filter has to be activated to suppress the howling component and stabilize the closed-loop system. The most commonly used notch filter structure in NHS is the second-order infinite impulse response (IIR), that is, biquadratic filter structure,

$$H_l(q,t) = \frac{b_l^{(0)}(t) + b_l^{(1)}(t)q^{-1} + b_l^{(2)}(t)q^{-2}}{1 + a_l^{(1)}(t)q^{-1} + a_l^{(2)}(t)q^{-2}}. \quad (3)$$

The bank of adjustable notch filters that is inserted in the electroacoustic forward path, as shown in Fig. 1, then consists of a cascade of $n_H/2$ such filters,

$$H(q,t) = \prod_{l=1}^{n_H/2} H_l(q,t) \quad (4)$$

with n_H the resulting order of the cascade filter.

The notch filter design procedure consists of two parts. First the set of design parameters $\mathcal{D}_H(t)$ provided by the howling detection algorithm has to be mapped to a set of filter specifications, which are then translated into filter coefficient values. A biquadratic notch filter has five coefficients, which depend on a set of five filter specifications [30]: the (angular) center frequency $\omega_{c,l}$, the (angular) bandwidth B_l, the notch gain $G_{c,l}$, the gain at dc $G_{0,l}$, and the gain at the Nyquist frequency $G_{\pi,l}$. If we fix the latter two variables to $G_{0,l} = G_{\pi,l} = 0$ dB, then only the first three filter specifications remain.

The set of design parameters $\mathcal{D}_H(t)$ should always contain the angular frequencies $\{\breve{\omega}_i\}_{i\in\mathcal{I}_H(t)}$ of the howling components that have been identified in the howling detection algorithm, where $\mathcal{I}_H(t) \subseteq \{1, \ldots, N\}$ denotes the set of indices for which howling has been detected. For each howling component a notch filter should be activated, with a center frequency corresponding to the howling frequency. The DFT magnitude values $\{|Y(\breve{\omega}_i)|\}_{i\in\mathcal{I}_H(t)}$ may also be contained in the set of design parameters $\mathcal{D}_H(t)$ since these values can be used to determine the notch gain $G_{c,l}$. However, it is common practice to work with fixed notch gain values that are independent of the howling component magnitude. This is a rather pragmatic choice, which allows the second part of the filter design procedure (that is, the translation of filter specifications to filter coefficients) to be executed off-line. Indeed given that the angular frequencies $\{\breve{\omega}_i\}_{i\in\mathcal{I}_H(t)}$ are restricted to the DFT frequency grid and the notch filter octave bandwidth is typically fixed (see hereafter), the coefficients for all possible notch filter designs can be calculated a priori if also the notch gain $G_{c,l}$ is restricted to a fixed set of values. The on-line effort in the second part of the notch filter design procedure then reduces to reading the corresponding filter coefficients from a lookup table in the NHS device memory. Typically when a new howling component has been detected (that is, a howling component at a frequency that has not occurred before), the notch gain is set to an initial value $G_{c,l}^{(0)}$, for example, $G_{c,l}^{(0)} = -3$ dB [12], [13] or $G_{c,l}^{(0)} = -6$ dB [19], [20]. If howling persists or

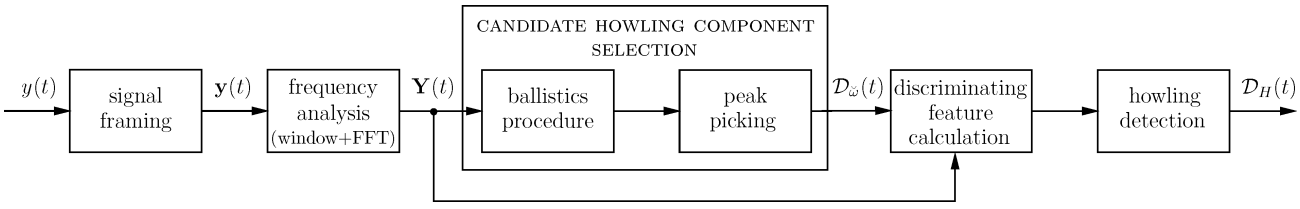

Fig. 2. NHS howling detection. From microphone signal $y(t)$ a set of notch filter design parameters $\mathcal{D}_H(t)$ is calculated.

reoccurs at a frequency close to a previously identified howling frequency, then the gain is decreased with $\Delta G_{c,l}$ dB, such as $\Delta G_{c,l} = -3$ dB [12], [13] or $\Delta G_{c,l} = -6$ dB [19], [20]. The angular notch filter bandwidth B_l is usually chosen proportional to the center frequency, such that the filter has a constant Q factor. The octave bandwidth is then also constant and is typically chosen in the range of 1/10–1/60 octave [12], [13], [22], [23].

Finally the filter specifications $\mathcal{S}_{H_l}(t) = \{\omega_{c,l}, B_l, G_{c,l}\}$ have to be translated to a set of filter coefficients $\mathcal{C}_{H_l}(t) = \{b_l^{(0)}(t), b_l^{(1)}(t), b_l^{(2)}(t), a_l^{(1)}(t), a_l^{(2)}(t)\}$. Most notch filter design methods are based on a bilinear transform of either an analog notch filter transfer function (see [31], [32]) or a digital notch filter transfer function centered at $\omega_c = \pi/2$ [33]. A novel design procedure for biquadratic notch filters has recently been proposed, which operates directly in the digital domain using a technique known as pole–zero placement [30], allowing for an equally accurate, yet more intuitive design. The complete notch-filter design procedure for the NHS method is shown schematically in Fig. 3.

2 SIGNAL FEATURES FOR HOWLING DETECTION

Six spectral and temporal features of the microphone signal have been proposed to classify candidate howling components with angular frequency $\breve{\omega}_i$ into howling components and source signal tonal components (that is, voiced speech or tonal audio components).

1) *Peak-to-Threshold Power Ratio (PTPR)* [14], [15], [19], [20]: A spectral feature that determines the ratio of the candidate howling component power $|Y(\breve{\omega}_i, t)|^2/M$ and a fixed absolute power threshold P_0,

$$\mathrm{PTPR}(\breve{\omega}_i, t) \quad [\mathrm{dB}] = 10 \log_{10} \frac{|Y(\breve{\omega}_i, t)|^2}{MP_0}. \tag{5}$$

The rationale behind using the PTPR for howling detection is that howling should only be suppressed when it appears with a minimum loudness [19], [20]. The absolute power threshold P_0 depends on the particular sound reinforcement scenario at hand. For example, a value of P_0 corresponding to a 85-dB sound pressure level was suggested in [19], [20] for a loudspeaker–microphone distance of 1 m.

2) *Peak-to-Average Power Ratio (PAPR)* [5], [6], [14]–[16], [18]–[25]: A spectral feature that determines the ratio of the candidate howling component power $|Y(\breve{\omega}_i, t)|^2/M$ and the average microphone signal power $\hat{P}_y(t)$,

$$\mathrm{PAPR}(\breve{\omega}_i, t) \quad [\mathrm{dB}] = 10 \log_{10} \frac{|Y(\breve{\omega}_i, t)|^2}{M\hat{P}_y(t)} \tag{6}$$

with

$$\hat{P}_y(t) = \frac{1}{M^2} \sum_{k=0}^{M-1} |Y(\omega_k, t)|^2. \tag{7}$$

This feature exploits the fact that howling may eventually have a large power compared to speech and audio components.

3) *Peak-to-Harmonic Power Ratio (PHPR)* [12]–[15]: A spectral feature that determines the ratio of the candidate howling component power $|Y(\breve{\omega}_i, t)|^2/M$ and its mth (sub)harmonic component power $|Y(m\breve{\omega}_i, t)|^2/M$,

$$\mathrm{PHPR}(\breve{\omega}_i, t, m) \quad [\mathrm{dB}] = 10 \log_{10} \frac{|Y(\breve{\omega}_i, t)|^2}{|Y(m\breve{\omega}_i, t)|^2}. \tag{8}$$

The existence of a harmonic spectral structure is a characteristic property of voiced speech and tonal audio components. Howling does not exhibit this structure, unless the amplifier or loudspeaker is driven into saturation.

4) *Peak-to-Neighboring Power Ratio (PNPR)* [4], [8]–[10]: A spectral feature that determines the ratio of the candidate howling component power $|Y(\breve{\omega}_i, t)|^2/M$ and its mth neighboring frequency component power $|Y(\breve{\omega}_i + 2\pi m/M, t)|^2/M$,

$$\mathrm{PNPR}(\breve{\omega}_i, t, m) \quad [\mathrm{dB}] = 10 \log_{10} \frac{|Y(\breve{\omega}_i, t)|^2}{|Y(\breve{\omega}_i + 2\pi m/M, t)|^2}. \tag{9}$$

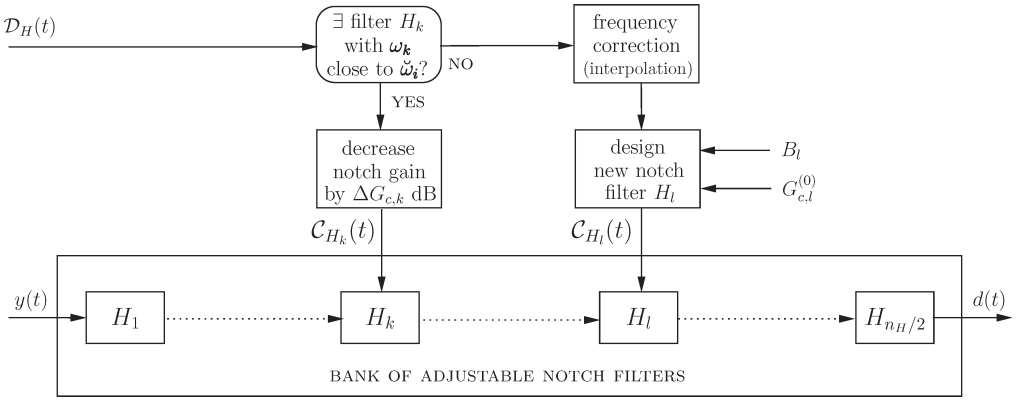

Fig. 3. NHS notch filter design. Microphone signal $y(t)$ is filtered in a bank of adjustable notch filters, designed using design parameters in $\mathcal{D}_H(t)$, resulting in howling-compensated signal $d(t)$.

Since voiced speech and tonal audio components can be represented as damped sinusoids, these components have a nonzero bandwidth and their power is spread over multiple DFT bins around a spectral peak. On the other hand howling is a purely sinusoidal signal, having its power concentrated in a single DFT bin (if appropriate windowing is applied).

5) *Interframe Peak Magnitude Persistence (IPMP)* [2], [3], [12], [13], [16], [18], [21]: A temporal feature based on counting the number of frames out of Q_M past signal frames, where the frequency $\breve{\omega}_i$ is in the set of candidate howling frequencies,

$$\mathrm{IPMP}(\breve{\omega}_i, t) = \frac{\sum_{j=0}^{Q_M-1} [\breve{\omega}_i \in \mathcal{D}_{\breve{\omega}}(t-jP)]}{Q_M}. \tag{10}$$

This feature relies on the observation that howling typically persists for a much longer time than voiced speech or tonal audio components.

6) *Interframe Magnitude Slope Deviation (IMSD)* [8]–[10]: A temporal feature that determines the deviation (over Q_M successive signal frames) of the slope, which is defined by averaging magnitude difference values of a candidate howling component, where the differentiation is carried out between an old signal frame and more recent signal frames,

$$\begin{aligned}\mathrm{IMSD}(\breve{\omega}_i, t) &= \frac{1}{Q_M-1}\sum_{m=1}^{Q_M-1}\left[\frac{1}{Q_M}\sum_{j=0}^{Q_M-1}\frac{1}{Q_M-j}\right.\\ &\quad\times(20\log_{10}|Y(\breve{\omega}_i, t-jP)|\\ &\quad\quad -20\log_{10}|Y(\breve{\omega}_i, t-Q_MP)|)\\ &\quad -\frac{1}{m}\sum_{j=0}^{m-1}\frac{1}{m-j}\\ &\quad\times(20\log_{10}|Y(\breve{\omega}_i, t-jP)|\\ &\quad\quad \left.-20\log_{10}|Y(\breve{\omega}_i, t-mP)|)\right].\end{aligned} \tag{11}$$

Small values for the IMSD are characteristic of howling components since these exhibit a nearly linear (dB scale) magnitude increase in time, hence a nearly constant slope can be expected.

3 EVALUATION OF HOWLING DETECTION CRITERIA

With the aim of objectively evaluating the performance of different howling detection criteria, we will describe the howling detection problem in a more formal way. Suppose that a howling detection experiment is carried out using a microphone signal consisting of L samples, such that $T_P = L/P$ microphone signal frames are available (with P the frame hop size). In each frame N candidate howling components are selected from the DFT magnitude spectrum by a peak picking algorithm. The howling detection procedure thus operates on a data set of T_PN spectral components, each of which may be considered as a different realization of a random process that either does or does not correspond to a howling component. When evaluating the detection performance, we assume that we know which of these T_PN components actually correspond to howling (positive realizations) or do not correspond to howling (negative realizations). By operating on the data set of T_PN components selected by the peak picking algorithm instead of on the entire set of DFT spectra (which would result in T_PM spectral components, with M the DFT size), the effect of the peak picking is actually excluded from the howling detection performance evaluation. Also the relative number of positive and negative realizations in the set of T_PN components can be balanced somewhat by properly choosing N.

For each of the T_PN spectral components in the data set, the corresponding howling detection problem can be formulated as a binary hypothesis test [26, ch. 3],

$\mathcal{H}_0$: howling does not occur (null hypothesis)
$\mathcal{H}_1$: howling does occur (alternative hypothesis).

The outcome of a howling detection criterion is either that the null hypothesis is rejected (howling is detected) or the null hypothesis is not rejected (howling is not detected). The probability of detection P_D for a certain howling detection criterion can then be defined as the probability that the null hypothesis is rejected for a positive realization,

$$P_\mathrm{D} = P(\mathcal{H}_1; \mathcal{H}_1). \tag{12}$$

This probability can be calculated by counting the number of "true positives" (N_TP), that is, the number of positive realizations in the data set for which the null hypothesis has been rejected, and dividing by the number of positive realizations in the data set N_P,

$$P_\mathrm{D} = \frac{N_\mathrm{TP}}{N_\mathrm{P}}. \tag{13}$$

On the other hand the probability of false alarm P_FA is defined as the probability that a certain howling detection criterion leads to the rejection of the null hypothesis for a negative realization,

$$P_\mathrm{FA} = P(\mathcal{H}_1; \mathcal{H}_0) \tag{14}$$

and can be calculated by dividing the number of "false positives" N_FP, that is, the number of negative realizations in the data set for which the null hypothesis has been rejected, by the number of negative realizations in the data set N_N,

$$P_\mathrm{FA} = \frac{N_\mathrm{FP}}{N_\mathrm{N}}. \tag{15}$$

A high probability of detection is required for the reliable operation of a sound reinforcement system, such that howling is quickly detected and suppressed by activating appropriate notch filters. On the other hand a

low probability of false alarm is beneficial to sound quality, since a false alarm may result in the suppression of a source signal tonal component. The tradeoff between P_D and P_{FA} is governed by the value of the detection threshold. An appropriate threshold value can be selected by plotting P_D versus P_{FA} for different threshold values, which results in the so-called receiver operating characteristic (ROC) curve [26, ch. 3]. The ROC curve can also be used to quantify the overall performance of a howling detection criterion, regardless of the threshold value, by calculating the area under the ROC curve (AUC) [34]. If N_T different threshold values are used to generate a (piecewise linear) ROC curve, then the AUC can be calculated,

$$\text{AUC} = \frac{1}{2}\sum_{k=2}^{N_T}[P_D(T_k) + P_D(T_{k-1})] \times [P_{FA}(T_k) - P_{FA}(T_{k-1})] \quad (16)$$

where the extreme threshold values T_1 and T_{N_T} should be chosen such that the ROC curve spans the entire unit square in the two-dimensional (P_{FA}, P_D) plane, that is, $P_D(T_1) = P_{FA}(T_1) = 0$ and $P_D(T_{N_T}) = P_{FA}(T_{N_T}) = 1$. In some cases, more particularly for some of the multiple-feature howling detection criteria described in Section 3.2, it is more appropriate to evaluate the AUC only for the lower part $[0, P_{FA}^{(\max)}]$ of the P_{FA} axis, for some $P_{FA}^{(\max)} < 1$. This leads to the so-called partial area under the ROC curve (PAUC) [35], which can be calculated as follows:

$$\text{PAUC} = \frac{1}{2P_{FA}^{(\max)}}\sum_{k=2}^{k^{(\max)}}[P_D(T_k) + P_D(T_{k-1})] \times [P_{FA}(T_k) - P_{FA}(T_{k-1})] + \frac{1}{2P_{FA}^{(\max)}} \times \left[P_D^{(\max)} + P_D(T_{k^{(\max)}})\right]\left[P_{FA}^{(\max)} - P_{FA}(T_{k^{(\max)}})\right] \quad (17)$$

where $k^{(\max)} \triangleq \max\{k | P_{FA}(T_k) \leq P_{FA}^{(\max)}\}$ and the probability of detection $P_D^{(\max)}$ corresponding to $P_{FA}^{(\max)}$ can be calculated by linear interpolation,

$$P_D^{(\max)} = P_D(T_{k^{(\max)}}) + \frac{P_D(T_{k^{(\max)}+1}) - P_D(T_{k^{(\max)}})}{P_{FA}(T_{k^{(\max)}+1}) - P_{FA}(T_{k^{(\max)}})}[P_{FA}^{(\max)} - P_{FA}(T_{k^{(\max)}})]. \quad (18)$$

Note that the PAUC definition in Eq. (17) includes a normalization factor $1/P_{FA}^{(\max)}$, which serves to scale the resulting PAUC value to the range [0, 1]. At the risk of being simplistic, we can state that the closer the AUC or PAUC value approaches unity, the better the corresponding detection criterion is expected to perform. For a more thorough statistical interpretation of the AUC we refer the interested reader to [36].

The ROC curves described hereafter have been generated from an experiment in which a closed-loop sound reinforcement system is simulated. In the simulation the feedback path $F(q, t)$ is a measured 100-ms room impulse response, the source signal is an audio signal fragment, more specifically a 10-s excerpt from the Partita No. 2 in D minor (Allemande) for solo violin by J. S. Bach, and the electroacoustic forward path $G(q, t)$ contains a broad-band gain cascaded with a saturation function. The gain factor is chosen slightly above the MSG, such that a single howling component slowly builds up in the microphone signal. The corresponding microphone signal spectrogram is shown in Fig. 4 (zooming in on the frequency region $f \in [0, 3]$ kHz). With $N = 3$ the data set contains $N_P = 166$ positive realizations and $N_N = 482$ negative realizations.

3.1 Single-Feature Howling Detection Criteria

Each of the six signal features described in Section 2 can be used to define a single-feature howling detection criterion. We should stress that these features have been defined such as to be invariant w.r.t. the frame length M and hop size P, and as a consequence the detection thresholds introduced in the following do not depend on the choice of M and P. The ROC curves corresponding to the single-feature howling detection criteria are shown in Fig. 5, and the AUC and PAUC values are given in the upper half of Table 1, where a value $P_{FA}^{(\max)} = 0.05$ is used to calculate the PAUC. Some of the detection criteria have been evaluated for different parameter values, in which case the optimal value (in terms of the highest AUC) has been boldfaced in Table 1.

1) PTPR criterion,

$$\text{PTPR}(\breve{\omega}_i, t) \geq T_{\text{PTPR}} \quad [\text{dB}] \Rightarrow \text{reject}\,\mathcal{H}_0. \quad (19)$$

The ROC curve for the PTPR criterion is shown in Fig. 5(a) for $T_{\text{PTPR}} \in (-\infty, +\infty)$ dB and $P_0 = 0$ dB.

2) PAPR criterion;

$$\text{PAPR}(\breve{\omega}_i, t) \geq T_{\text{PAPR}} \quad [\text{dB}] \Rightarrow \text{reject}\,\mathcal{H}_0. \quad (20)$$

The PAPR criterion is probably the most widely used howling detection criterion, and different values for the threshold have been proposed, such as $T_{\text{PAPR}} = 6$ dB [5], [6], $T_{\text{PAPR}} = 10\log_{10}(M/150)^2$ dB [19], [20], and $T_{\text{PAPR}} = 10$ dB [21]. The ROC curve for the PAPR criterion is shown in Fig. 5(b) for $T_{\text{PAPR}} \in (-\infty, +\infty)$ dB.

3) PHPR criterion,[2]

$$\bigwedge_{m \in \mathcal{M}_{\text{PHPR}}} [\text{PHPR}(\breve{\omega}_i, t, m) \geq T_{\text{PHPR}}[\text{dB}]] \Rightarrow \text{reject}\,\mathcal{H}_0. \quad (21)$$

In this criterion multiple PHPR features are combined for different harmonic indices m. In [12], [13] howling detection is performed with $\mathcal{M}_{\text{PHPR}} = \{0.5, 1.5, 2, 3, 4\}$ and $T_{\text{PHPR}} = 33$ dB, whereas in [14], [15] a simpler PHPR criterion is used with $\mathcal{M}_{\text{PHPR}} = \{2\}$. The ROC curves for

[2]Here the logical conjuction (AND) operator for two or more Boolean variables is defined as follows: $\wedge_i x_i$ is true if and only if all variables x_i are true.

the PHPR criterion are shown in Fig. 5(c) for $T_{\mathrm{PHPR}} \in (-\infty, +\infty)$ dB and for different choices of $\mathcal{M}_{\mathrm{PHPR}}$. It appears that the use of subharmonics (that is, $m \in \{0.5, 1.5\}$) is not beneficial to the detection performance. The PHPR criterion yields the largest AUC among all single-feature howling detection criteria.

4) PNPR criterion,

$$\bigwedge_{m\in\mathcal{M}_{\mathrm{PNPR}}} [\mathrm{PNPR}(\breve{\omega}_i, t, m) \geq T_{\mathrm{PNPR}}[\mathrm{dB}]] \Rightarrow \text{reject}\,\mathcal{H}_0. \tag{22}$$

The PNPR criterion incorporates multiple PNPR features, calculated for different neighboring frequency bins around a candidate howling component. In [4] different thresholds $T_{\mathrm{PNPR}}(|m|)$ were used for different neighbors, with $\mathcal{M}_{\mathrm{PNPR}} = \{\pm 1, \pm 2\}$. The ROC curves for the PNPR criterion are shown in Fig. 5(d) for $T_{\mathrm{PNPR}} \in (-\infty, +\infty)$ dB and for different choices of $\mathcal{M}_{\mathrm{PNPR}}$. In the threshold range where the ROC curves fall below the dotted diagonal line, the PNPR criterion is not appropriate since $P_{\mathrm{FA}} > P_{\mathrm{D}}$. We should stress that the use of the direct neighbors on either side of the candidate howling component ($m = \pm 1$) generally degrades the PNPR detection performance, as can be seen from Fig. 5(d) and Table 1. This is due to the spectral leakage of high-power howling components into neighboring DFT bins, which may occur even when DFT windowing is used.

5) IPMP criterion,

$$\mathrm{IPMP}(\breve{\omega}_i, t) \geq T_{\mathrm{IPMP}} \Rightarrow \text{reject}\,\mathcal{H}_0. \tag{23}$$

The IPMP threshold is usually chosen as $T_{\mathrm{IPMP}} = 1$ [2], [3], [16], [18], [21] with, for example, $Q_M = 3$ [21]. In [12], [13] howling detection is performed with $T_{\mathrm{IPMP}} = 3/5$ and $Q_M = 5$. The ROC curves for the IPMP criterion are shown in Fig. 5(e) for $T_{\mathrm{IPMP}} \in \{0, 1/Q_M, \ldots, (Q_M + 1)/Q_M\}$ and for different choices of Q_M.

6) IMSD criterion,

$$|\mathrm{IMSD}(\breve{\omega}_i, t)| \leq T_{\mathrm{IMSD}}[\mathrm{dB}] \Rightarrow \text{reject}\,\mathcal{H}_0. \tag{24}$$

A detection threshold $T_{\mathrm{IMSD}} = 0.05$ dB has been proposed in [8], with $Q_M = 7$. The ROC curves for the IMSD criterion are shown in Fig. 5(f) for $T_{\mathrm{IMSD}} \in [0, +\infty)$ dB and for different choices of Q_M.

3.2 Multiple-Feature Howling Detection Criteria

Multiple signal features can be combined straightforwardly to obtain howling detection criteria that perform better than the single-feature criteria described. We first briefly mention two existing multiple-feature criteria and then show how improved multiple-feature criteria can be derived by using the information in the ROC curves shown in Fig. 5.

In [12], [13] a multiple-feature howling detection criterion based on the PHPR and IPMP features is proposed,

$$\left(\bigwedge_{m\in\mathcal{M}_{\mathrm{PHPR}}} [\mathrm{PHPR}(\breve{\omega}_i, t, m) \geq T_{\mathrm{PHPR}}(\mathrm{dB})]\right) \wedge (\mathrm{IPMP}(\breve{\omega}_i, t) \geq T_{\mathrm{IPMP}}) \Rightarrow \text{reject}\,\mathcal{H}_0 \tag{25}$$

with $\mathcal{M}_{\mathrm{PHPR}} = \{0.5, 1.5, 2, 3, 4\}$ and $Q_M = 5$. The ROC curves for this criterion, corresponding to different values of T_{IPMP}, are shown in Fig. 6(a) for $T_{\mathrm{PHPR}} \in (-\infty, +\infty)$, whereas the AUC and PAUC values are given in the lower half of Table 1. Note that for $T_{\mathrm{IPMP}} > 0$ there is no value of T_{PHPR} for which $P_{\mathrm{D}} = P_{\mathrm{FA}} = 1$, and hence an AUC value cannot be calculated since the ROC curve does not span the

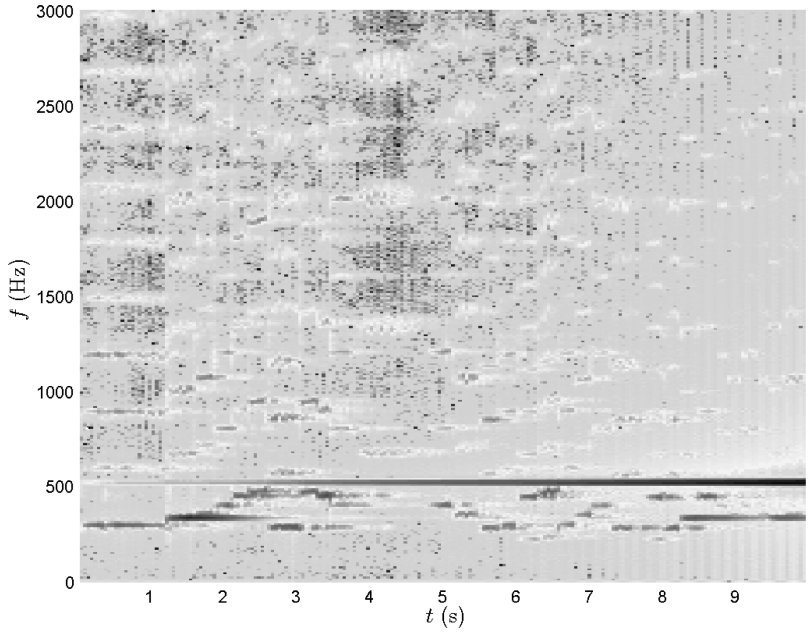

Fig. 4. Microphone signal spectrogram after feeding an audio source signal to a simulated unstable closed-loop system (zooming in on frequency region $f \in [0, 3]$ kHz).

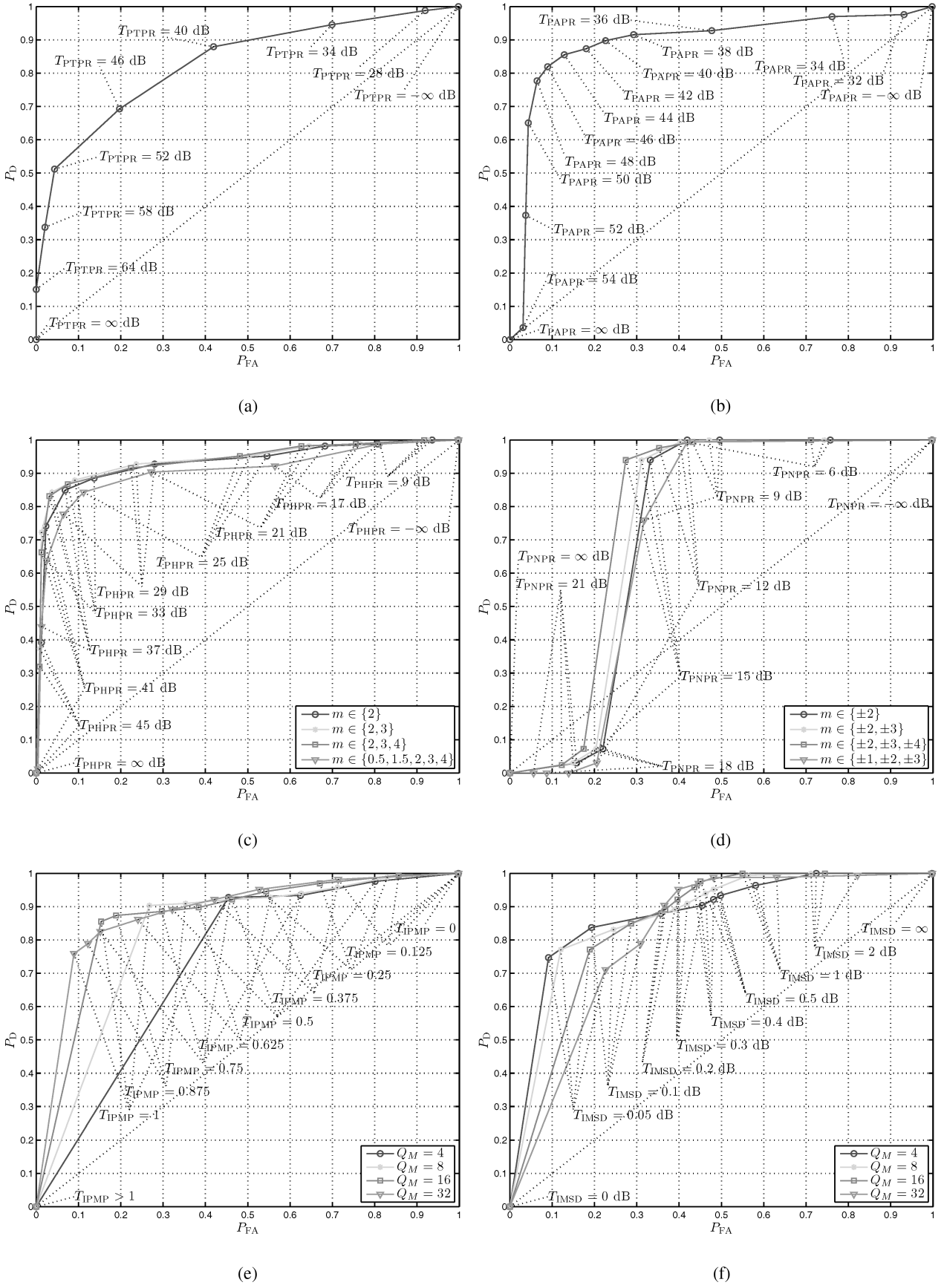

Fig. 5. ROC curves for single-feature howling detection criteria. (a) PTPR criterion. (b) PAPR criterion. (c) PHPR criterion. (d) PNPR criterion. (e) IPMP criterion. (f) IMSD criterion.

Table 1. Comparison of area under ROC curve (AUC) and partial AUC (PAUC) for $P_{\mathrm{FA}}^{(\max)} = 5\%$.

Criterion	AUC	PAUC	Parameter and Threshold Values	
PTPR	**0.83**	0.36	$P_0 = 0$ dB	
PAPR	**0.89**	0.19		
PHPR	0.93	0.59	$\mathcal{M}_{\mathrm{PHPR}} = \{2\}$	
	0.94	0.68	$\boldsymbol{\mathcal{M}_{\mathrm{PHPR}} = \{2, 3\}}$	
	0.94	0.66	$\mathcal{M}_{\mathrm{PHPR}} = \{2, 3, 4\}$	
	0.90	0.52	$\mathcal{M}_{\mathrm{PHPR}} = \{0.5, 1.5, 2, 3, 4\}$	
PNPR	0.73	0.00	$\mathcal{M}_{\mathrm{PNPR}} = \{\pm 2\}$	
	0.74	0.00	$\mathcal{M}_{\mathrm{PNPR}} = \{\pm 2, \pm 3\}$	
	0.77	0.00	$\boldsymbol{\mathcal{M}_{\mathrm{PNPR}} = \{\pm 2, \pm 3, \pm 4\}}$	
	0.71	0.00	$\mathcal{M}_{\mathrm{PNPR}} = \{\pm 1, \pm 2, \pm 3\}$	
IPMP	0.73	0.05	$Q_M = 4$	
	0.81	0.08	$Q_M = 8$	
	0.86	0.14	$Q_M = 16$	
	0.88	0.21	$\boldsymbol{Q_M = 32}$	
IMSD	**0.88**	0.20	$\boldsymbol{Q_M = 4}$	
	0.87	0.16	$Q_M = 8$	
	0.85	0.10	$Q_M = 16$	
	0.81	0.08	$Q_M = 32$	
PHPR & IPMP [12], [13]	0.91	0.54	$T_{\mathrm{IPMP}} = 0$	$\mathcal{M}_{\mathrm{PHPR}} = \{0.5, 1.5, 2, 3, 4\}$, $Q_M = 5$
	N/A	0.58	$T_{\mathrm{IPMP}} = 2/5$	
	N/A	**0.60**	$\boldsymbol{T_{\mathrm{IPMP}} = 1}$	
FEP [8]–[10]	0.94	0.76	$Q_M = 8$	
	0.98	**0.90**	$\boldsymbol{Q_M = 16}$	
	0.94	0.74	$Q_M = 32$	
PHPR & PNPR	0.94	0.66	$T_{\mathrm{PNPR}} = -\infty$ dB	$\mathcal{M}_{\mathrm{PHPR}} = \{2, 3\}$, $\mathcal{M}_{\mathrm{PNPR}} = \{\pm 2, \pm 3, \pm 4\}$
	N/A	0.67	$T_{\mathrm{PNPR}} = 6$ dB	
	N/A	**0.68**	$\boldsymbol{T_{\mathrm{PNPR}} = 8}$ **dB**	
PHPR & IMSD	N/A	**0.84**	$\boldsymbol{T_{\mathrm{IMSD}} = 0.5}$ **dB**	$\mathcal{M}_{\mathrm{PHPR}} = \{2, 3\}$, $Q_M = 16$
	N/A	0.83	$T_{\mathrm{IMSD}} = 1$ dB	
	0.94	0.66	$T_{\mathrm{IMSD}} = \infty$ dB	
PNPR & IMSD	N/A	**0.58**	$\boldsymbol{T_{\mathrm{IMSD}} = 0.5}$ **dB**	$\mathcal{M}_{\mathrm{PNPR}} = \{\pm 2, \pm 3, \pm 4\}$, $Q_M = 16$
	N/A	0.11	$T_{\mathrm{IMSD}} = 1$ dB	
	N/A	0.01	$T_{\mathrm{IMSD}} = 2$ dB	
	0.78	0.00	$T_{\mathrm{IMSD}} = \infty$ dB	
PHPR & PNPR & IMSD	N/A	0.83	$T_{\mathrm{PNPR}} = -\infty$ dB	$\mathcal{M}_{\mathrm{PHPR}} = \{2, 3\}$, $\mathcal{M}_{\mathrm{PNPR}} = \{\pm 2, \pm 3, \pm 4\}$, $Q_M = 16$, $T_{\mathrm{IMSD}} = 0.5$ dB
	N/A	0.85	$T_{\mathrm{PNPR}} = 6$ dB	
	N/A	0.88	$T_{\mathrm{PNPR}} = 7$ dB	
	N/A	**0.92**	$\boldsymbol{T_{\mathrm{PNPR}} = 8}$ **dB**	

entire unit square. This is exactly the reason for having introduced the PAUC measure in Eq. (17). Comparing the ROC curve for this criterion with the ROC curve for the PHPR criterion in Fig. 5(c), and the corresponding (P)AUC values, it can be observed that there is only a slight benefit in adding the IPMP feature to the PHPR criterion.

A different multiple-feature howling detection criterion was proposed in [8]–[10] and consists in defining a so-called feedback existence probability (FEP) criterion,

$$\mathrm{FEP}(\breve{\omega}_i, t) \geq T_{\mathrm{FEP}} \Rightarrow \text{reject}\,\mathcal{H}_0 \tag{26}$$

with

$$\begin{aligned}\mathrm{FEP}(\breve{\omega}_i, t) = {} & 0.7 \cdot \mathrm{slopeness}(\breve{\omega}_i, t) + 0.3 \\ & \cdot \mathrm{peakness}(\breve{\omega}_i, t).\end{aligned} \tag{27}$$

The peakness feature was defined in [8]–[10] to reflect the time-averaged probability (over eight signal frames) that the PNPR, averaged over 6 neighboring frequency bins on either side of $\breve{\omega}_i$ (excluding the closest neighbor on either side), exceeds a 15-dB threshold, that is,

$$\begin{aligned}&\mathrm{peakness}(\breve{\omega}_i, t) \\ &= \frac{1}{16}\sum_{j=0}^{7}\left\{\left[\frac{1}{6}\sum_{m=2}^{7}\mathrm{PNPR}(\breve{\omega}_i, t-jP, m) \geq 15\,\mathrm{dB}\right]\right. \\ &\qquad \left.+\left[\frac{1}{6}\sum_{m=-7}^{-2}\mathrm{PNPR}(\breve{\omega}_i, t-jP, m) \geq 15\,\mathrm{dB}\right]\right\}.\end{aligned} \tag{28}$$

The slopeness feature is related to the IMSD feature following a nonlinear mapping (which is not explicitly given in [8]–[10]. Hence we use $\mathrm{slopeness}(\breve{\omega}_i,\ t) = \mathrm{e}^{-|\mathrm{IMSD}(\breve{\omega}_i, t)|}$). The ROC curves obtained with different values for Q_M are shown in Fig. 6(b) for $T_{\mathrm{FEP}} \in [0, 1]$, and the (P)AUC values are given in the lower half of Table 1. The FEP criterion clearly performs better than the single-feature PNPR and IMSD criteria.

To derive alternative multiple-feature howling detection criteria, two objectives should be kept in mind. As mentioned, while a high probability of false alarm results in poor sound quality due to the unnecessary activation of notch filters, a low probability of detection may also lead to poor sound quality because of howling. Moreover the closed-loop system stability can be guaranteed only when a high probability of detection is achieved. This suggests that in terms of the overall acoustic feedback control performance, a high probability of detection should be considered more important than a low probability of false alarm. A second issue is that when combining different criteria using a logical conjunction (that is, the $\wedge$ operator), the probability of detection of the multiple-feature criterion can never be greater than the probability of detection obtained with the corresponding single-feature criteria. Instead the effect of a logical conjunction is that the probability of false alarm will decrease compared to the single-feature criteria. As a consequence we should focus on combining single-feature howling detection criteria that yield a high probability of detection, regardless of their probability of false alarm.

From this perspective, and by observing the single-feature ROC curves in Fig. 5, we can conclude that in particular the PNPR and IMSD features (and, to a lesser extent, the PHPR feature) are well suited for use in a multiple-feature howling detection criterion. In this way three novel criteria are obtained by pairwise logical conjunction of the PHPR, PNPR, and IMSD criteria given in Eqs. (21), (22), and (24), respectively, and an additional three-feature criterion results from combining all three PHPR, PNPR, and IMSD features. The corresponding ROC curves are shown in Fig. 7, and the (P)AUC values are given in the lower half of Table 1. In

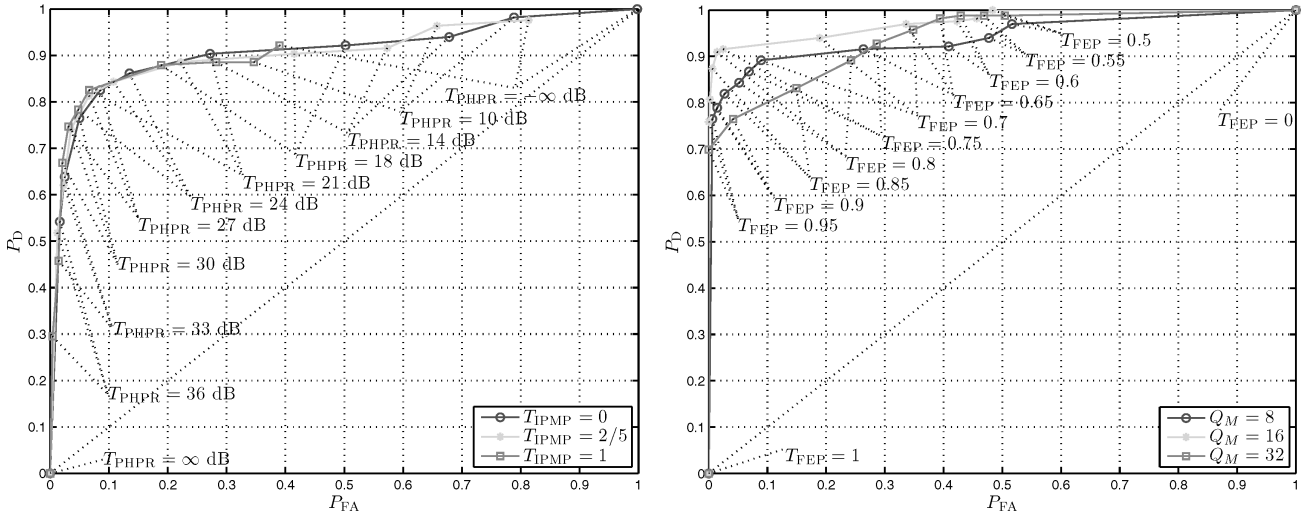

(a) (b)

Fig. 6. ROC curves for existing multiple-feature howling detection criteria. (a) PHPR & IPMP criterion [12], [13]. (b) FEP criterion [8]–[10].

each of the four cases the multiple-feature howling detection criterion clearly outperforms the corresponding single-feature criteria. For the PHPR & PNPR criterion the improvement is only visible at higher P_{FA} values, whereas the other three criteria show also an improvement in the lower P_{FA} range (which is clearly visible from the PAUC values in Table 1). Except for the PNPR & IMSD criterion, the novel howling detection criteria outperform the existing PHPR & IPMP criterion [12], [13] in terms of the PAUC, whereas only the PHPR & PNPR & IMSD criterion results in a higher PAUC value than the existing FEP criterion [8]–[10].

By means of the AUC and PAUC measures the detection performance of the different single-feature and multiple-feature howling detection criteria can be compared regardless of the threshold values used. On the other hand we can also compare the detection performance of the different criteria for one particular choice of the threshold values. One such comparison is given in Table 2, where the probability of false alarm of the different criteria is calculated for a threshold value that results in a 95% probability of detection. The parameter and threshold values used to obtain these results are also given. It can be seen that with the novel multiple-feature criteria the probability of false alarm can be reduced drastically: $P_{FA} = 5\%$ for the PNPR & IMSD criterion and $P_{FA} = 3\%$ for the PHPR & PNPR & IMSD criterion.

Finally we compare the different howling detection criteria in terms of their computational complexity. Following the block scheme in Fig. 2, the number of real multiplications for the entire howling detection procedure in one signal frame can be decomposed into four contributions,

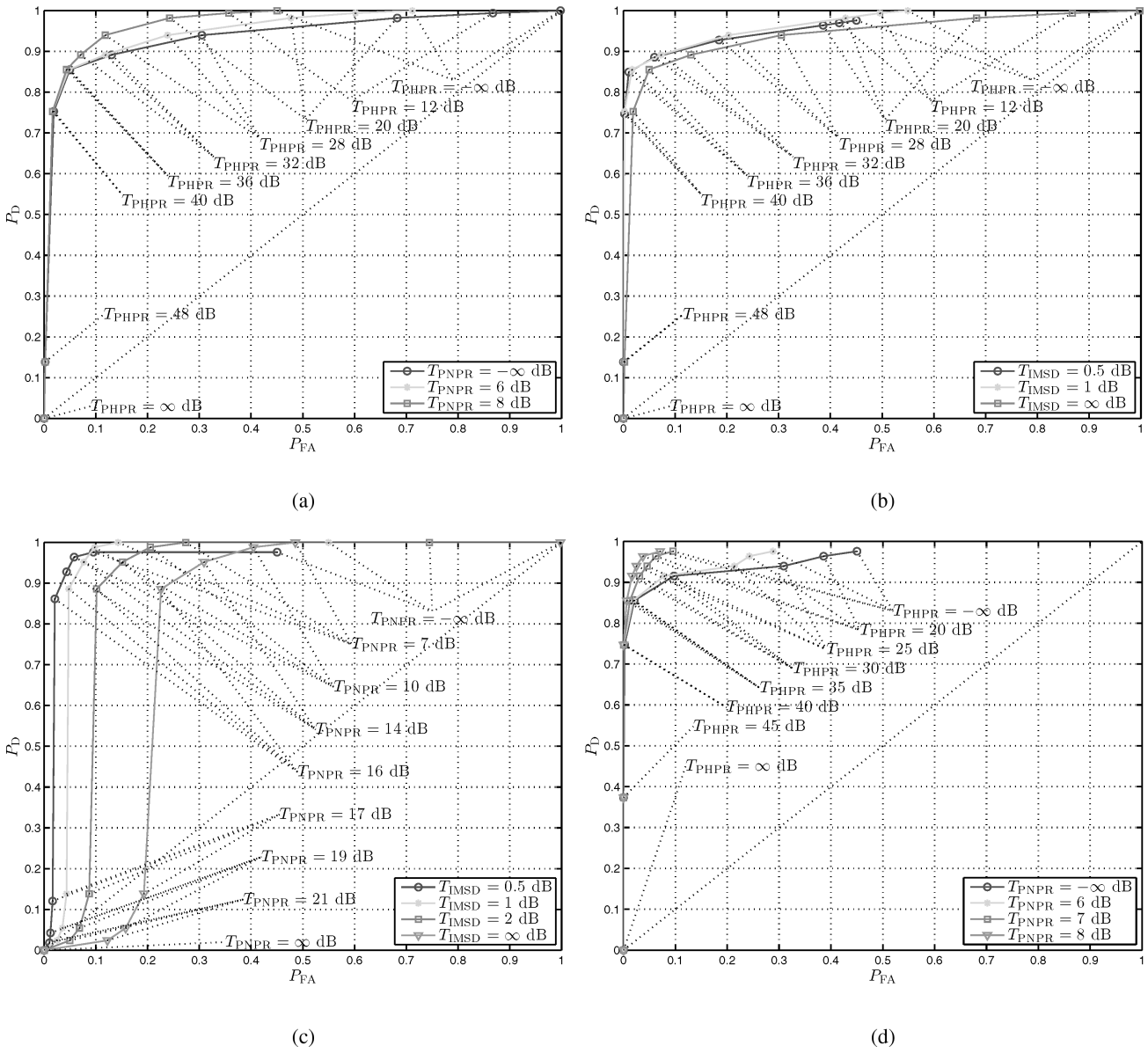

Fig. 7. ROC curves for novel multiple-feature howling detection criteria. (a) PHPR & PNPR criterion. (b) PHPR & IMSD criterion. (c) PNPR & IMSD criterion. (d) PHPR & PNPR & IMSD criterion.

$$\mathbb{M} = \underbrace{M + O(M \log_2 M)}_{\text{frequency analysis}} + \underbrace{N \cdot O(M/2)}_{\text{candidate selection}} + \underbrace{\mathbb{M}_F}_{\text{feature calculation}} + \underbrace{\mathbb{M}_D}_{\text{howling detection}} \quad (29)$$

where the first two contributions are common to the different criteria. Expressions for the latter two contributions in Eq. (29) are given in Table 3, where the set cardinality $|\cdot|$ denotes the number of elements in a set. In the rightmost column of Table 3, the sum of $\mathbb{M}_F$ and $\mathbb{M}_D$ is evaluated for the parameter values given in Table 2. Note that the spectral features (PTPR, PAPR, PHPR, and PNPR) are significantly cheaper to calculate than the temporal features (IPMP and IMSD). As for the multiple-feature howling detection criteria, the FEP criterion [8]–[10] is somewhat more expensive than the other ones, whereas criteria not involving the IMSD feature are significantly cheaper. Depending on the choice of the frame size M, the relative importance of the last two terms $\mathbb{M}_F$ and $\mathbb{M}_D$ in the total number of multiplications in Eq. (29) may vary considerably: for $M = 4096$ (as used throughout this paper) these terms do not contribute significantly, whereas for $M = 128$ (as used, for example, in [8]–[10]) the sum $\mathbb{M}_F + \mathbb{M}_D$ may account for more than half of the total computational complexity.

Table 2. Comparison of probability of false alarm for $P_D = 95\%$.

Criterion	P_{FA}	Parameter and Threshold Values
PTPR	70%	$P_0 = 0$ dB, $T_{PTPR} = 34$ dB
PAPR	63%	$T_{PAPR} = 35$ dB
PHPR	37%	$\mathcal{M}_{PHPR} = \{2, 3\}$, $T_{PHPR} = 27$ dB
PNPR	31%	$\mathcal{M}_{PNPR} = \{\pm2, \pm3, \pm4\}$, $T_{PNPR} = 14$ dB
IPMP	53%	$Q_M = 32$, $T_{IPMP} = 8/32$
IMSD	40%	$Q_M = 32$, $T_{IMSD} = 0.3$ dB
PHPR & IPMP [12], [13]	65%	$\mathcal{M}_{PHPR} = \{0.5, 1.5, 2, 3, 4\}$, $T_{PHPR} = 10$ dB, $Q_M = 5$, $T_{IPMP} = 2/5$
FEP [8]–[10]	24%	$Q_M = 16$, $T_{FEP} = 0.68$
PHPR & PNPR	15%	$\mathcal{M}_{PHPR} = \{2, 3\}$, $T_{PHPR} = 26$ dB, $\mathcal{M}_{PNPR} = \{\pm2, \pm3, \pm4\}$, $T_{PNPR} = 8$ dB
PHPR & IMSD	25%	$\mathcal{M}_{PHPR} = \{2, 3\}$, $T_{PHPR} = 27$ dB, $Q_M = 16$, $T_{IMSD} = 1$ dB
PNPR & IMSD	5%	$\mathcal{M}_{PNPR} = \{\pm2, \pm3, \pm4\}$, $T_{PNPR} = 12$ dB, $Q_M = 16$, $T_{IMSD} = 0.5$ dB
PHPR & PNPR & IMSD	3%	$\mathcal{M}_{PHPR} = \{2, 3\}$, $T_{PHPR} = 23$ dB, $\mathcal{M}_{PNPR} = \{\pm2, \pm3, \pm4\}$, $T_{PNPR} = 8$ dB, $Q_M = 16$, $T_{IMSD} = 0.5$ dB

Table 3. Comparison of number of real multiplications for feature calculation ($\mathbb{M}_F$) and howling detection ($\mathbb{M}_D$).

Criterion	$\mathbb{M}_F$	$\mathbb{M}_D$	$\mathbb{M}_F + \mathbb{M}_D$
PTPR	$3N$	N	12
PAPR	$4N$	N	15
PHPR	$3N\lvert\mathcal{M}_{PHPR}\rvert$	$N(2\lvert\mathcal{M}_{PHPR}\rvert - 1)$	27
PNPR	$3N\lvert\mathcal{M}_{PNPR}\rvert$	$N(2\lvert\mathcal{M}_{PNPR}\rvert - 1)$	87
IPMP	$N(Q_M N + 1)$	N	294
IMSD	$N\left(\frac{3}{2}Q_M^2 + \frac{5}{2}Q_M + 1\right)$	$2N$	4857
PHPR & IPMP [12], [13]	$N(3\lvert\mathcal{M}_{PHPR}\rvert + Q_M N + 1)$	$N(2\lvert\mathcal{M}_{PHPR}\rvert + 1)$	126
FEP [8]–[10]	$N\left(\frac{3}{2}Q_M^2 + \frac{5}{2}Q_M + 46\right)$	N	1413
PHPR & PNPR	$3N(\lvert\mathcal{M}_{PHPR}\rvert + \lvert\mathcal{M}_{PNPR}\rvert 1)$	$N(2\lvert\mathcal{M}_{PHPR}\rvert + 2\lvert\mathcal{M}_{PNPR}\rvert - 1)$	117
PHPR & IMSD	$N\left(3\lvert\mathcal{M}_{PHPR}\rvert + \frac{3}{2}Q_M^2 + \frac{5}{2}Q_M + 1\right)$	$2N(\lvert\mathcal{M}_{PHPR}\rvert + 1)$	1311
PNPR & IMSD	$N\left(3\lvert\mathcal{M}_{PNPR}\rvert + \frac{3}{2}Q_M^2 + \frac{5}{2}Q_M + 1\right)$	$2N(\lvert\mathcal{M}_{PNPR}\rvert + 1)$	1371
PHPR & PNPR & IMSD	$N\left(3\lvert\mathcal{M}_{PHPR}\rvert + 3\lvert\mathcal{M}_{PNPR}\rvert + \frac{3}{2}Q_M^2 + \frac{5}{2}Q_M + 1\right)$	$2N(\lvert\mathcal{M}_{PHPR}\rvert + \lvert\mathcal{M}_{PNPR}\rvert + 1)$	1401

4 NHS SIMULATION RESULTS

A selection of the existing and novel howling detection criteria presented in the preceding has been evaluated in a number of NHS computer simulations. Each simulation consists of four equally long phases, as shown in Fig. 8. In the first phase the electroacoustic forward path gain is set to a value K_1 that would result in a 3-dB gain margin if no acoustic feedback control were performed. In the second phase the gain $20 \log_{10} K(t)$ is then increased linearly up to a value of $20 \log_{10} K_2 = 20 \log_{10} K_1 + \Delta K$ beyond the point of instability, with $\Delta K = 5$ dB. In the third and fourth phases the gain is fixed to K_2, and at the end of the third phase an acoustic feedback path change due to a 1-m displacement of the microphone is simulated. The source signal is a 60-s audio signal, taken from the same recording as the signal shown in Fig. 4.

In [1] it was observed that a satisfactory NHS performance is obtained only when the howling detection threshold is chosen so as to yield an extremely low probability of false alarm. This observation can be explained by noting that the deactivation of notch filters is an open problem in the NHS literature. As a consequence every false alarm results in the unnecessary activation of a notch filter, which remains active until the end of the simulation. Not only does this affect the sound quality, but it also reduces the number of available notch filters that can be applied when howling does occur. Following this observation we only include those howling detection criteria in the NHS simulations that are capable of achieving a relatively high probability of detection ($P_D > 85\%$) at a probability of false alarm as low as $P_{FA} = 1\%$. The included criteria are the FEP criterion [8]–[10] (with $Q_M = 16$), the PHPR & IMSD criterion (with $\mathcal{M}_{PHPR} = \{2, 3\}$ and $Q_M = 16$), and the PHPR & PNPR & IMSD criterion (with $\mathcal{M}_{PHPR} = \{2, 3\}$, $\mathcal{M}_{PNPR} = \{\pm 2, \pm 3, \pm 4\}$, and $Q_M = 16$). Each of these criteria has been evaluated for three different combinations of the corresponding threshold values, with the aim of illustrating the effect of too high a probability of false alarm or too low a probability of detection on the NHS performance.

In the left-hand graphs of Fig. 9, the instantaneous MSG obtained with an NHS method employing the selected howling detection criteria is plotted as a function of time. The instantaneous MSG is defined as,[3]

$$\mathrm{MSG}(t) \quad [\mathrm{dB}] = -20 \log_{10} \left[\max_{\omega \in \mathcal{P}} |H(\omega, t) F(\omega, t)| \right] \quad (30)$$

where $H(\omega, t)$ and $F(\omega, t)$ represent the short-term frequency response of the bank of notch filters and the acoustic feedback path, respectively, and $\mathcal{P}$ denotes the set of frequencies at which the loop phase $\angle H(\omega, t) F(\omega, t)$ is an integer multiple of 2π. The instantaneous electroacoustic forward path gain $20 \log_{10} K(t)$ is also plotted in Fig. 9, as are the MSG values obtained without acoustic feedback control, with MSG $F_1(q)$ and MSG $F_2(q)$ denoting the MSG before and after the acoustic feedback path change, respectively. In the time interval where $20 \log_{10} K(t) < \mathrm{MSG}\ F_1(q)$ (that is, for $0\ \mathrm{s} \leq t \leq 23\ \mathrm{s}$) the sound reinforcement system is guaranteed to be stable; hence ideally no howling should be detected. An MSG curve that does exhibit "jumps" during this time interval, indicates the occurrence of false alarms and the consequent activation of unnecessary notch filters, which may cause source signal degradations. This effect can be observed particularly in the star-marked line MSG curves in Fig. 9, which correspond to the most loose choice of

[3]Here we assume that the electroacoustic forward path solely consists of a broad-band gain, that is, $G(q, t) \equiv K(t)$. We refer to [1] for a more general MSG definition.

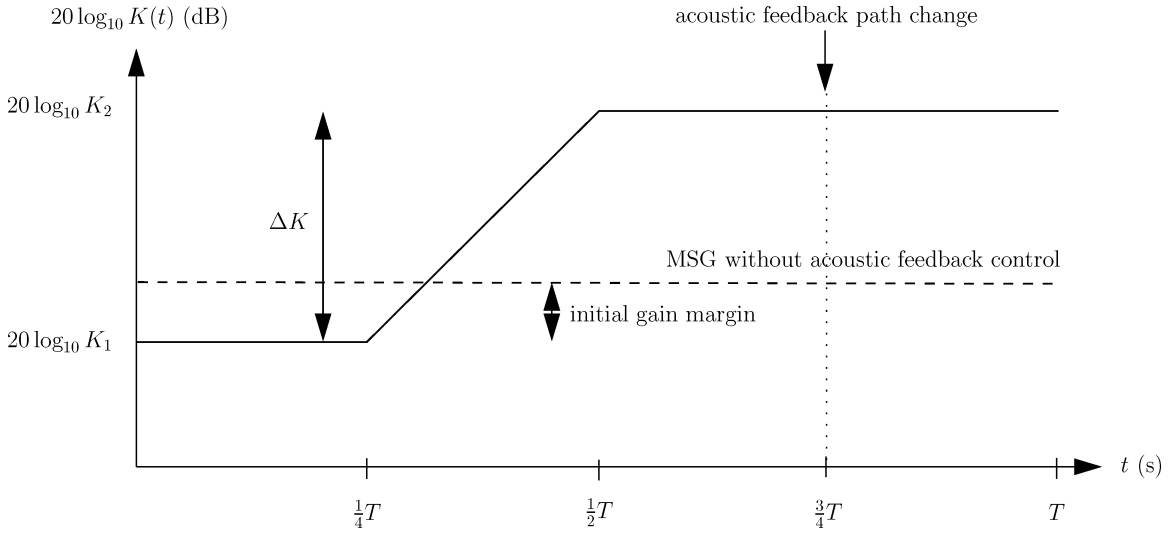

Fig. 8. NHS simulation layout. Electroacoustic forward path gain $20 \log_{10} K(t)$ versus time.

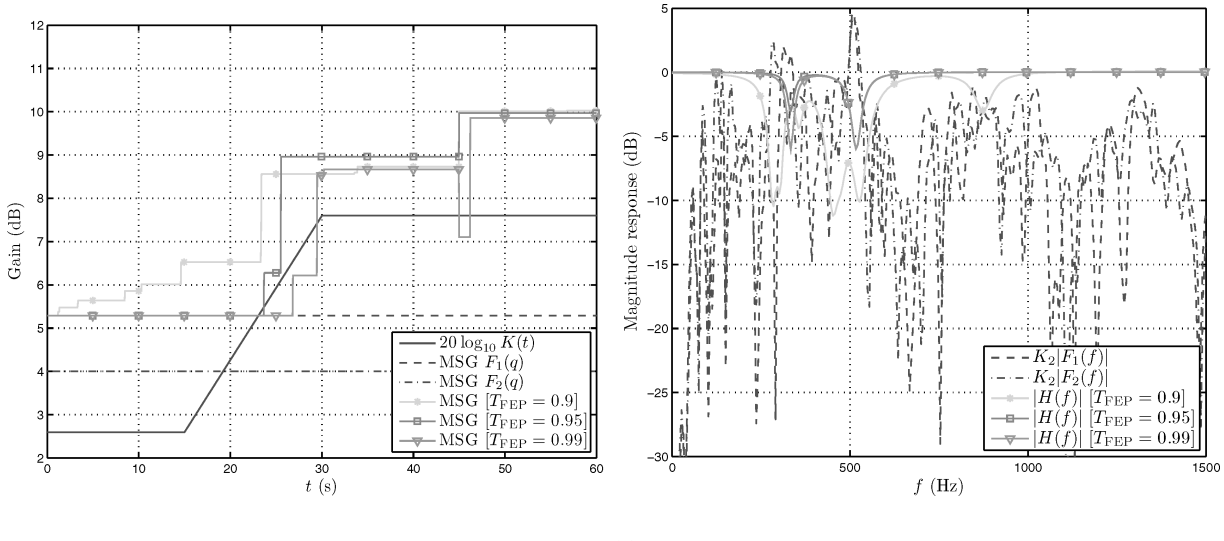

(a)

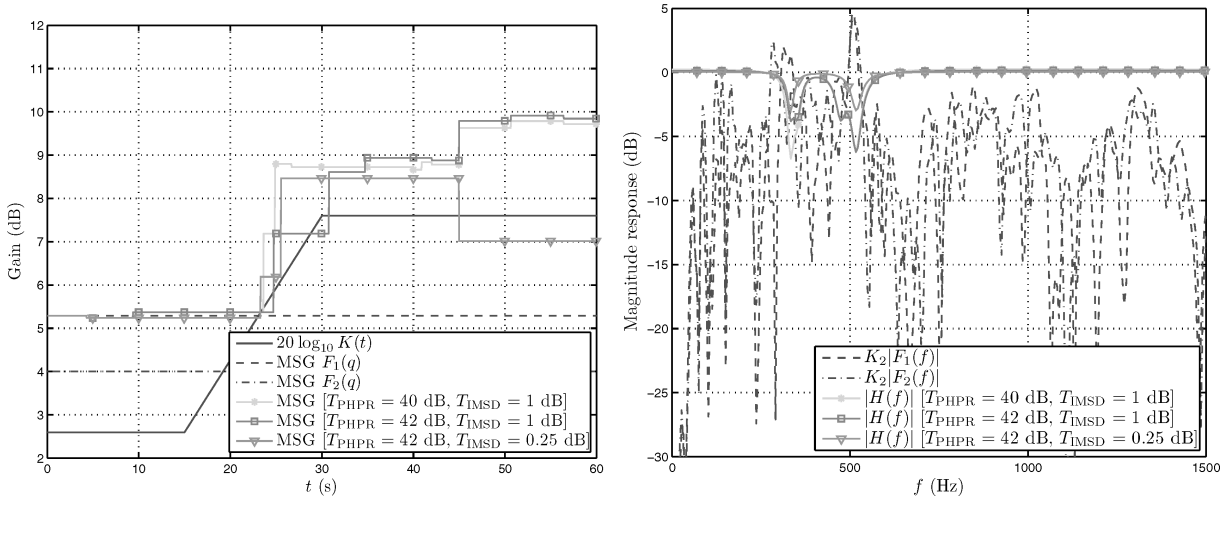

(b)

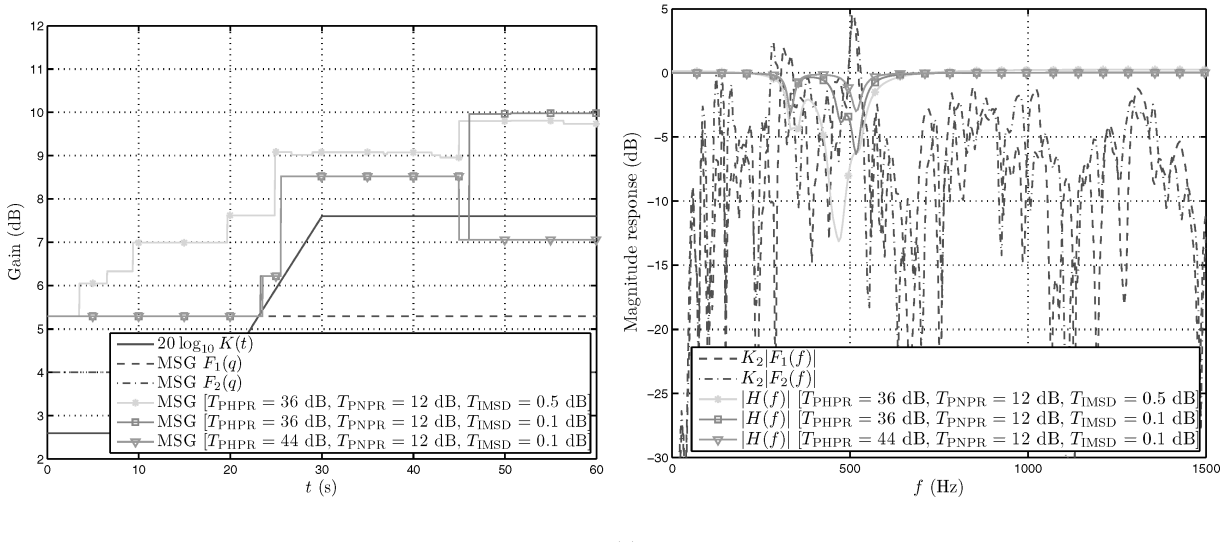

(c)

Fig. 9. NHS simulation results. Instantaneous MSG versus time (left) and final bank of notch filter response (right). (a) FEP criterion [8]–[10]. (b) PHPR & IMSD criterion. (c) PHPR & PNPR & IMSD criterion.

the threshold values. When the electroacoustic forward path gain is increased, the MSG curves are expected to increase correspondingly due to the proper activation of notch filters. As long as the instantaneous MSG curve stays above the instantaneous gain curve, stability can be guaranteed. This is not the case for the triangle-marked line MSG curves in Fig. 9, where too strict a choice of the threshold values leads to an unacceptably large detection lag, which in turn results in a perceptible howling effect. After the feedback path change at $t = 45$ s the MSG may drop below the instantaneous gain curve, after which it ideally jumps up again, thereby indicating the proper adaptation of the NHS method to the new situation.

In the right-hand graphs of Fig. 9 we have plotted the magnitude response $|H(f)|$ of the bank of notch filters at the end of each simulation ($t = T = 60$ s) together with the loop gain responses $K_2|F_1(f)|$ and $K_2|F_2(f)|$ obtained without acoustic feedback control. Ideally the notch filters should compensate exactly for the resonances in frequency regions where the loop gain exceeds the 0-dB level (in particular in regions [277, 298], [307, 340], and [495, 530] Hz). However, we should stress that the loop phase (which is not shown here) also determines the occurrence of howling and hence the activation of notch filters. It can be observed from the notch filter responses in Fig. 9 that a relatively loose choice of the detection threshold values (corresponding to the star-marked line magnitude response curves) leads to the use of notch filters with an overly large notch depth as well as the activation of notch filters at noncritical frequencies. On the other hand too strict a choice of the threshold values (corresponding to the triangle-marked line magnitude response curves) may result in the design of notch filters with insufficient notch depth.

Finally a number of performance measures has been calculated with the aim of evaluating the overall NHS performance in terms of the achievable amplification, sound quality, and reliability when employing the selected howling detection criteria. The achievable amplification is quantified by two opposing measures, namely, the final MSG increase

$$\Delta\text{MSG} \quad [\text{dB}] = -20\log_{10}\left[\frac{\max_{\omega\in\mathcal{P}}|H(\omega,T)F(\omega,T)|}{\max_{\omega\in\mathcal{P}}|F(\omega,T)|}\right] \tag{31}$$

and the cumulated notch gain at the end of the simulation ($t = T = 60$ s), defined as $\sum_{l=1}^{n_H/2} G_{c,l}$. Ideally an NHS method should succeed in combining a high MSG increase with a minimal cumulated notch gain, such as to avoid source signal degradation. The sound quality is quantified using a frequency-weighted log-spectral signal distortion (SD) measure, which was proposed in the context of the real-time evaluation of adaptive feedback cancellation algorithms in hearing aids [37] and is defined as

$$\text{SD}(t) = \sqrt{\int_0^{f_s/2} w_{\text{ERB}}(f)\left[10\log_{10}\frac{S_d(f,t)}{S_v(f,t)}\right]^2 df} \tag{32}$$

where $S_d(f, t)$ and $S_v(f, t)$ denote the short-term power spectral density (PSD) of the howling-compensated signal and source signal (see Fig. 1), respectively, and $w_{\text{ERB}}(f)$ is a weighting function that gives equal weight to each auditory critical band in the Nyquist interval, following Table 2 of the ANSI standard S3.5-1997 [38]. We will evaluate the mean SD, averaged over the time interval 30 s $\leq t \leq 60$ s, which corresponds to the preferential mode of operation of the sound reinforcement system (because it allows for a high electroacoustic forward path gain). Finally the reliability is also quantified by two opposing measures, namely, the detection lag T_D, defined as the (average) length of the time interval(s) during which the instantaneous MSG is below the instantaneous electroacoustic forward path gain, and the number of false alarms N_{FA}, defined as the number of times that a notch filter is activated (or its notch depth is increased) when the instantaneous MSG is at least 2 dB above the instantaneous electroacoustic forward path gain. With the 2-dB margin applied in the definition of N_{FA}, we aim to avoid that a notch filter activation due to ringing (which may occur when the gain is 2 dB or less below the MSG [39]) is counted as a false alarm.

Table 4 contains the values of the performance measures defined in the preceding. The measure values obtained with the best choice of threshold values are shown in bold for each of the three howling detection criteria under consideration. We can observe that the performance of the FEP [8]–[10] and PHPR & PNPR & IMSD criteria is rather similar, whereas the PHPR & IMSD criterion suffers from a relatively high number of false alarms (and, correspondingly, a large cumulated notch gain) and a worse detection lag. The lightface measure values in Table 4 confirm the intuition that too loose a choice of the threshold values only improves the detection lag at the cost of a large cumulated notch gain, whereas too strict a choice reduces the number of false alarms at the cost of a significantly higher detection lag. In both cases the resulting effect on sound quality may be detrimental.

The howling-compensated signals obtained in the simulations are available for download,[4] such that the sound quality can be assessed subjectively by the reader.

5 CONCLUSION

The aim of this paper has been to evaluate existing criteria for howling detection in notch-filter-based howling suppression (NHS) and to propose alternative criteria that are particularly suited for audio NHS applications involving music signals. Six existing signal features have been defined in a formal way, and the detection performance of the corresponding single-feature criteria has been evaluated by analyzing the receiver operating characteristic (ROC) curves. Multiple-feature

[4] ftp://ftp.esat.kuleuven.be/pub/sista/vanwaterschoot/abstracts/09-207.html.

howling detection criteria have then been defined by a logical conjunction of single-feature criteria of which each exhibits a sufficiently high probability of detection. As a result novel howling detection criteria have been obtained that allow for a drastic decrease of the probability of false alarm for a fixed probability of detection. While the minimum probability of false alarm at $P_D = 95\%$ with existing criteria was found to be 33% for single-feature and 24% for multiple-feature criteria, the novel criteria can achieve a P_{FA} value as low as 3%. In addition the proposed PHPR & PNPR & IMSD criterion has been found to exhibit a slight increase in the partial area under the ROC curve (PAUC) as compared to the FEP criterion [8]–[10], while computationally it is somewhat less complex. Finally a selection of existing and novel howling detection criteria has been evaluated in a number of NHS simulations in terms of the achievable amplification, sound quality, and reliability. The simulation results indicate in particular the importance of a proper choice of the detection threshold values and the resulting impact on sound quality.

6 ACKNOWLEDGMENT

This research work was carried out at the ESAT Laboratory of Katholieke Universiteit Leuven, in the frame of K.U.Leuven Research Council CoE EF/05/006 ("Optimization in Engineering, OPTEC"), the Belgian Program on Interuniversity Attraction Poles initiated by the Belgian Federal Science Policy Office IUAP P6/04 (DYSCO, "Dynamical systems, control and optimization", 2007–2011), the Concerted Research Action GOA-AMBioRICS, and Research Project FWO G.0600.08 ("Signal processing and network design for wireless acoustic sensor networks"), and was supported by the Institute for the Promotion of Innovation through Science and Technology in Flanders (IWT-Vlaanderen).

7 REFERENCES

[1] T. van Waterschoot and M. Moonen, "Fifty Years of Acoustic Feedback Control: State of the Art and Future Challenges," *Proc. IEEE*, to be published.

[2] E. T. Patronis, Jr., "Acoustic Feedback Detector and Automatic Gain Control," U.S. patent 4,079,199 (1978 Mar.).

[3] E. T. Patronis, Jr., "Electronic Detection of Acoustic Feedback and Automatic Sound System Gain Control," *J. Audio Eng. Soc.*, vol. 26, pp. 323–326 (1978 May).

[4] S. Ando, "Howling Detection and Prevention Circuit and a Loudspeaker System Employing the Same," U.S. patent 6,252,969 (2001 June).

[5] M. Hanajima, M. Yoneda, and T. Okuma, "Howling Eliminator," WIPO patent appl. WO/1999/021 396 (1999 Apr.).

[6] M. Hanajima, M. Yoneda, and T. Okuma, ''Howling Eliminating Apparatus,'' U.S. patent 6,125,187 (2000 Sept.).

[7] Y. Terada and A. Murase, "Howling Control Device and Howling Control Method," U.S. patent 7,190,800 (2007 Mar.).

[8] N. Osmanovic, V. E. Clarke, and E. Velandia, "An In-Flight Low Latency Acoustic Feedback Cancellation Algorithm," presented at the 123rd Convention of the

Table 4. Performance measures for NHS simulations.

Criterion (Parameter Values)	Amplification		Sound Quality [mean(SD)]	Reliability		Threshold Values
	ΔMSG	$\Sigma_l G_{c,l}$		T_D	N_{FA}	
FEP [8]–[10] ($Q_M = 16$)	6.0 dB	−42 dB	4.7 dB	0 s	9	$T_{FEP} = 0.9$
	6.0 dB	**−9 dB**	**4.1 dB**	**0.6 s**	**0**	$\boldsymbol{T_{FEP} = 0.95}$
	5.9 dB	−12 dB	4.5 dB	3.8 s	0	$T_{FEP} = 0.99$
PHPR & IMSD ($\mathcal{M}_{PHPR} = \{2, 3\}$, $Q_M = 16$)	5.7 dB	−33 dB	4.3 dB	0.2 s	6	$T_{PHPR} = 40$ dB, $T_{IMSD} = 1$ dB
	5.8 dB	**−24 dB**	**4.3 dB**	**1.6 s**	**4**	$\boldsymbol{T_{PHPR} = 42}$ **dB,** $\boldsymbol{T_{IMSD} = 1}$ **dB**
	3.0 dB	−9 dB	29.0 dB	7.6 s	1	$T_{PHPR} = 42$ dB, $T_{IMSD} = 0.25$ dB
PHPR & PNPR & IMSD ($\mathcal{M}_{PHPR} = \{2, 3\}$, $Q_M = 16$, $\mathcal{M}_{PNPR} = \{\pm 2, \pm 3, \pm 4\}$)	5.7 dB	−39 dB	4.6 dB	0 s	7	$T_{PHPR} = 36$ dB, $T_{PNPR} = 12$ dB, $T_{IMSD} = 0.5$ dB
	6.0 dB	**−12 dB**	**4.6 dB**	**0.6 s**	**1**	$\boldsymbol{T_{PHPR} = 36}$ **dB,** $\boldsymbol{T_{PNPR} = 12}$ **dB,** $\boldsymbol{T_{IMSD} = 0.1}$ **dB**
	3.1 dB	−6 dB	28.8 dB	7.7 s	0	$T_{PHPR} = 44$ dB, $T_{PNPR} = 12$ dB, $T_{IMSD} = 0.1$ dB

Audio Engineering Society, *J. Audio Eng. Soc. (Abstracts)*, www.aes.org/events/123/123rdWrapUp.pdf, (2007 Oct.), convention paper 7266.

[9] N. Osmanovic and V. Clarke, "Acoustic Feedback Cancellation System," WIPO patent appl. WO/2007/013 981 (2007 Feb.).

[10] N. Osmanovic and V. Clarke, "Acoustic Feedback Cancellation System," U.S. patent 7,664,275 (2010 Feb.).

[11] J. B. Foley, "Adaptive Periodic Noise Cancellation for the Control of Acoustic Howling," in *Proc. IEE Colloq. on Adaptive Filters* (London, UK, 1989 Mar.), pp. 7/1–7/4.

[12] D. M. Oster, M. P. Lewis, and T. J. Tucker, "Method and Apparatus for Adaptive Audio Resonant Frequency Filtering," WIPO patent appl. WO/1991/020 134 (1991 Dec.).

[13] M. P. Lewis, T. J. Tucker, and D. M. Oster, "Method and Apparatus for Adaptive Audio Resonant Frequency Filtering," U.S. patent 5,245,665 (1993 Sept.).

[14] M. H. Er, T. H. Ooi, L. S. Li, and C. J. Liew, "A DSP-Based Acoustic Feedback Canceller for Public Address Systems," in *Proc. Int. Conf. on Signal Processing (ICSP '93)* (Beijing, China, 1993 Oct.), pp. 1251–1254.

[15] M. H. Er, T. H. Ooi, L. S. Li, and C. J. Liew, "A DSP-Based Acoustic Feedback Canceller for Public Address Systems," *Microprocessors and Microsys*., vol. 18, pp. 39–47 (1994 Jan./Feb.).

[16] A. Kawamura, M. Matsumoto, M. Serikawa, and H. Numazu, "Sound Amplifying Apparatus with Automatic Howl-Suppressing Function," U.S. patent 5,442,712 (1995 Aug.).

[17] R. Porayath and D. J. Mapes-Riordan, "Acoustic Feedback Elimination Using Adaptive Notch Filter Algorithm," U.S. patent 5,999,631 (1999 Dec.).

[18] A. Kawamura, M. Matsumoto, M. Serikawa, and H. Numazu, "Sound Amplifying Apparatus with Automatic Howl-Suppressing Function," Euro. patent EP0 599 450 (2001 Nov.).

[19] P. R. Williams, "Method and System for Elimination of Acoustic Feedback," WIPO patent appl. WO/2002/021 817 (2002 Mar.).

[20] P. R. Williams, "Method and System for Elimination of Acoustic Feedback," U.S. patent appl. 2010/0 046 768 A1 (2010 Feb.).

[21] A. F. Rocha and A. J. S. Ferreira, "An Accurate Method of Detection and Cancellation of Multiple Acoustic Feedbacks," presented at the 118th Convention of the Audio Engineering Society, *J. Audio Eng. Soc. (Abstracts)*, vol. 53, p. 663 (2005 July/Aug.), convention paper 6335.

[22] M. Börsch, "Method for Constraining Electroacoustic Feedback," Euro. patent appl. EP1 684 543 A1 (2006 July).

[23] M. Börsch, "Method for Suppressing Electroacoustic Feedback," U.S. patent appl. 2006/0 159 282 A1 (2006 July).

[24] D. Somasundaram, "Feedback Cancellation in a Sound System," Euro. patent appl. EP1 903 833 A1 (2008 Mar.).

[25] D. Somasundaram, "Feedback Cancellation in a Sound System," U.S. patent appl. 2008/0 085 013 A1 (2008 Apr.).

[26] S. M. Kay, *Fundamentals of Statistical Signal Processing: Detection Theory* (Prentice-Hall, Upper Saddle River, NJ, 1998).

[27] F. J. Harris, "On the Use of Windows for Harmonic Analysis with the Discrete Fourier Transform," *Proc. IEEE*, vol. 66, pp. 51–83 (1978 Jan.).

[28] J. O. Smith, "Mathematics of the Discrete Fourier Transform (DFT)," http://ccrma.stanford.edu/~jos/mdft/ (accessed 2008 Nov.).

[29] F. Keiler and S. Marchand, "Survey on Extraction of Sinusoids in Stationary Sounds," in *Proc. 5th Int. Conf. on Digital Audio Effects (DAFx '02)* (Hamburg, Germany, 2002 Sept.), pp. 51–58.

[30] T. van Waterschoot and M. Moonen, "A Pole–Zero Placement Technique for Designing Second-Order IIR Parametric Equalizer Filters," *IEEE Trans. Audio, Speech. Lang. Process*., vol. 15, pp. 2561–2565 (2007 Nov.).

[31] P. A. Regalia and S. K. Mitra, "Tunable Digital Frequency Response Equalization Filters," *IEEE Trans. Acoust., Speech, Signal Process*., vol. ASSP-35, pp. 118–120 (1987 Jan.).

[32] R. Bristow-Johnson, "The Equivalence of Various Methods of Computing Biquad Coefficients for Audio Parametric Equalizers," presented at the 97th Convention of the Audio Engineering Society, *J. Audio Eng. Soc. (Abstracts),* vol. 42, pp. 1062, 1063 (1994 Dec.), preprint 3906.

[33] J. A. Moorer, "The Manifold Joys of Conformal Mapping: Applications of Digital Filtering in the Studio," *J. Audio Eng. Soc*., vol. 31, pp. 826–841 (1983 Nov.).

[34] T. Fawcett, "An Introduction to ROC Analysis," *Pattern Recogn. Lett*., vol. 27, pp. 861–874 (2006 June), special issue on ROC analysis in pattern recognition.

[35] L. E. Dodd and M. S. Pepe, "Partial AUC Estimation and Regression," *Biometrics*, vol. 59, pp. 614–623 (2003 Sept.).

[36] J. A. Hanley and B. J. McNeil, "The Meaning and Use of the Area Under a Receiver Operating Characteristic (ROC) Curve," *Radiology*, vol. 143, pp. 29–36 (1982 Apr.).

[37] A. Spriet, K. Eneman, M. Moonen, and J. Wouters, "Objective Measures for Real-Time Evaluation of Adaptive Feedback Cancellation Algorithms in Hearing Aids," in *Proc. 16th Euro. Signal Processing Conf. (EUSIPCO '08)* (Lausanne, Switzerland, 2008 Aug.).

[38] ANSI S3.5–1987, "American National Standard Methods for Calculation of the Speech Intelligibility Index," Am. Nat. Stds. Inst., New York (1997).

[39] M. R. Schroeder, "Improvement of Acoustic-Feedback Stability by Frequency Shifting," *J. Acoust. Soc. Am*., vol. 36, pp. 1718–1724 (1964 Sept.).

THE AUTHORS

T. van Waterschoot

M. Moonen

Toon van Waterschoot was born in Lier, Belgium, on June 11, 1979. He received a Master's degree and a Ph.D. degree in electrical engineering from Katholieke Universiteit Leuven (K. U. Leuven), Leuven, Belgium, in 2001 and 2009, respectively.

In 2002 he spent a year as teaching assistant with the Antwerp Maritime Academy, Belgium. From 2002 to 2003 and from 2008 to 2009 he was a research assistant with K. U. Leuven, and from 2004 to 2007 he was a research assistant with the Institute for the Promotion of Innovation through Science and Technology in Flanders (IWT), Belgium. After his Ph.D. graduation he was a postdoctoral research fellow with K. U. Leuven, and since 2010 he has been a postdoctoral research fellow with Delft University of Technology (TU Delft), The Netherlands. Since 2005 he has also been a visiting teaching assistant at the Advanced Learning and Research Institute of the Univesrity of Lugano, Switzerland, where he is teaching digital signal processing.

Dr. van Waterschoot served as TPC track chair for speech processing at the 18th European Signal Processing Conference (EUSIPCO-2010) and has been a technical reviewer and TPC member for numerous journals and conferences. His research interests are in adaptive signal processing and parameter estimation, with application to acoustic signal enhancement, speech and audio processing, and wireless communications.

●

Marc Moonen received an electrical engineering degree and a Ph.D. degree in applied sciences from Katholieke Universiteit Leuven (K. U. Leuven), Belgium, in 1986 and 1990, respectively.

Since 2004 he has been a full professor in the Electrical Engineering Department of K. U. Leuven, where he is heading a research team working in the areas of numerical algorithms and signal processing for digital communications, wireless communications, DSL, and audio signal processing.

Dr. Moonen received the 1994 K. U. Leuven Research Council Award, the 1997 Alcatel Bell (Belgium) Award (with Piet Vandaele), the 2004 Alcatel Bell (Belgium) Award (with Raphael Cendrillon), and was a 1997 Laureate of the Belgium Royal Academy of Science. He received a journal best paper award from the *IEEE Transactions on Signal Processing* (with Geert Leus) and from *Elsevier Signal Processing* (with Simon Doclo). He was chair of the IEEE Benelux Signal Processing Chapter and is currently past-president of EURASIP (European Association for Signal Processing) and a member of the IEEE Signal Processing Society Technical Committee on Signal Processing for Communications. He has served as editor-in-chief for the *EURASIP Journal on Applied Signal Processing* and has been a member of the editorial board of the *IEEE Transactions on Circuits and Systems II,* the *IEEE Signal Processing Magazine,* and *Integration, the VLSI Journal*. He is currently a member of the editorial board of *EURASIP Journal on Applied Signal Processing, EURASIP Journal on Wireless Communications and Networking,* and *Signal Processing*.